

1995

## Surface Recombination Velocity and Bulk Carrier Lifetime Measurement of Silicon Crystals by Using Photoluminescence Time Decay

Karsten Thölmann  
*Toshiba Corporation*

Masakazu Yamaguchi  
*Toshiba Corporation*

Akihiro Yahata  
*Toshiba Corporation*

Follow this and additional works at: <https://digitalcommons.usu.edu/microscopy>



Part of the [Biology Commons](#)

### Recommended Citation

Thölmann, Karsten; Yamaguchi, Masakazu; and Yahata, Akihiro (1995) "Surface Recombination Velocity and Bulk Carrier Lifetime Measurement of Silicon Crystals by Using Photoluminescence Time Decay," *Scanning Microscopy*. Vol. 1995 : No. 9 , Article 10.

Available at: <https://digitalcommons.usu.edu/microscopy/vol1995/iss9/10>

This Article is brought to you for free and open access by the Western Dairy Center at DigitalCommons@USU. It has been accepted for inclusion in Scanning Microscopy by an authorized administrator of DigitalCommons@USU. For more information, please contact [digitalcommons@usu.edu](mailto:digitalcommons@usu.edu).



## SURFACE RECOMBINATION VELOCITY AND BULK CARRIER LIFETIME MEASUREMENT OF SILICON CRYSTALS BY USING PHOTOLUMINESCENCE TIME DECAY

Karsten Thölmann\*, Masakazu Yamaguchi and Akihiro Yahata

Research and Development Center, Toshiba Corporation, 1 Komukai Toshiba-cho, Saiwai-ku, Kawasaki 210, Japan

### Abstract

The time decay for photoluminescence (PL) emitted from silicon crystals has been used to obtain both bulk carrier lifetime ( $\tau_b$ ) and surface recombination velocity (S). Experimental results were interpreted with the assumptions that the sample was under a low-excitation condition and that the ratio of radiative to non-radiative recombination rates was constant throughout the carrier decay process. Analysis was applied to several wafers covered with different kinds of silicon dioxide (SiO<sub>2</sub>). The results indicate that PL time decay measurement is effective to obtain the values of  $\tau_b$  and S.

**Key Words:** Simulation, photoluminescence, silicon, carrier lifetime, surface recombination velocity, laser, algorithm.

### Introduction

Both bulk carrier lifetime ( $\tau_b$ ) and surface recombination velocity (S) are very important physical parameters of silicon (Si) crystals which possibly determine the characteristics of Si devices [4]. Therefore, convenient methods for obtaining both  $\tau_b$  and S have been the subject of recent investigations [2, 3]. Recently, Buczkowski *et al.* [1] developed an algorithm to obtain both parameters for bare and oxidized Czochralski Si material, which was based on a microwave absorption/ reflection measurements. The samples, however, to which that technique can be applied, are limited. For example, the specific resistivity and the carrier lifetime need to be higher than 1  $\Omega\text{cm}$  and 1  $\mu\text{s}$ , respectively, and the diameter of the measured region needs to be as large as 1 mm. Therefore, the technique, which can obtain both parameters for all kinds of Si crystals, has been earnestly required.

The photoluminescence (PL) time decay measurement has been developed to investigate carrier lifetime depth profiles for Si devices because the diameter of the measured region can be as small as 100  $\mu\text{m}$  [7]. Furthermore, this technique has little limitations concerning with both specific resistivity and carrier lifetime for the sample. Therefore, it is desirable to obtain both  $\tau_b$  and S by using PL time decay measurement. In the present work, we present an algorithm to obtain both parameters, which is based on PL time decay measurement, and also results for several kinds of Si crystals, obtained by using that algorithm.

### Experimental and Simulation Method

The PL time decay method has been little used in measuring the carrier lifetime of Si crystals, except in the case of highly doped materials [6], because the PL intensity from Si crystals is very weak and photomultiplier (PM) sensitivity is very poor at the PL peak wavelength. These problems have been overcome by using a powerful light source, a nitrogen laser.

Figure 1 shows a schematic view of the carrier life-

\*Address for correspondence and present address:  
Karsten Thölmann  
SIBET GmbH, Research & Development,  
Garbsener Landstrasse 10,  
D-30419 Hannover,  
Germany

Telephone number: (49)-511-277-1738  
FAX number: (49)-511-277-2710

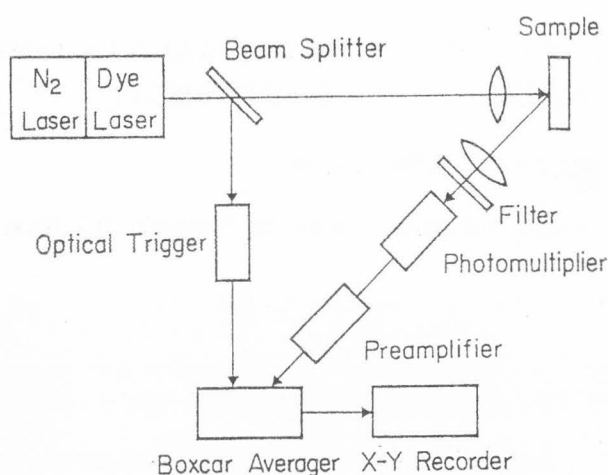


Figure 1. Schematic view of the carrier lifetime measurement instrument.

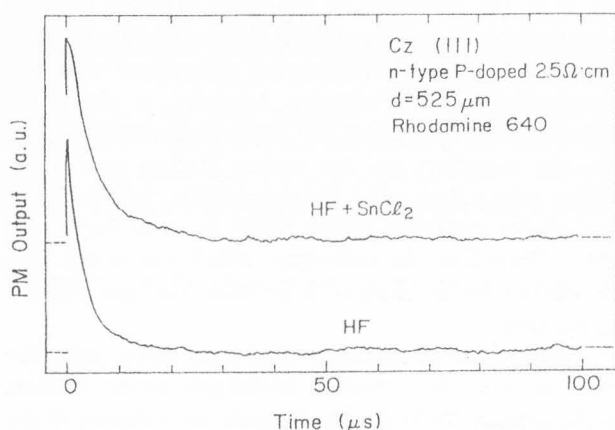


Figure 2. PL time decay curves for P-doped n-type Si wafers.

time measurement instrument at the initial stage. The wavelength of the nitrogen laser is 337.1 nm, the pulse energy {at 2 pulses per second (pps)} is 2.5 mJ, the peak energy (at 2 pps) is 500 kW, the pulse width is 4 to 8 ns, the average output (at 10 pps) is 24 mW, and the repetition rate (maximum) is 20 pps. Rhodamine 640 was used as the dye laser material excited by the nitrogen laser. The output of the dye laser is several percent that of the nitrogen laser. The wavelength of the dye laser is 640 nm. The output of the dye laser is divided into two beams: one excites the Si crystal sample, whereas the other excites the pin diode of an optical trigger. The PL from the excited sample is introduced into the PM. Laser light is blocked by a filter in front of the PM. The output from the PM is amplified by a quick-response preamplifier and, together with the trigger signal from the optical trigger, introduced into a

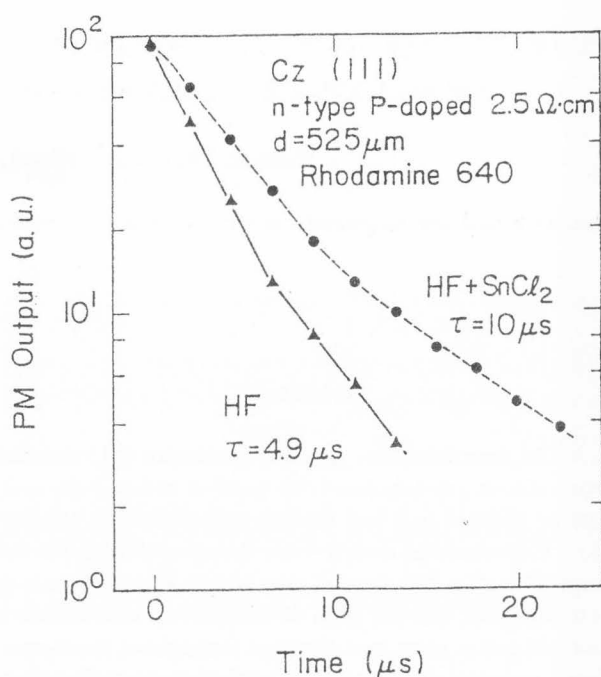


Figure 3. PL time decay curves for the same samples as in Figure 2, with vertical axis plotted on a logarithmic scale.

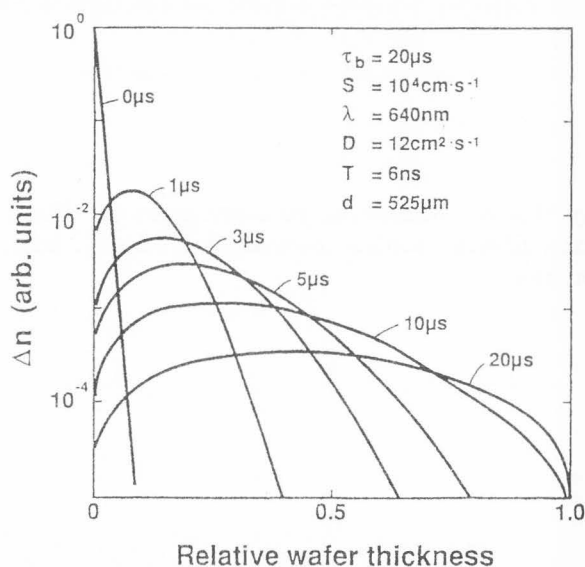
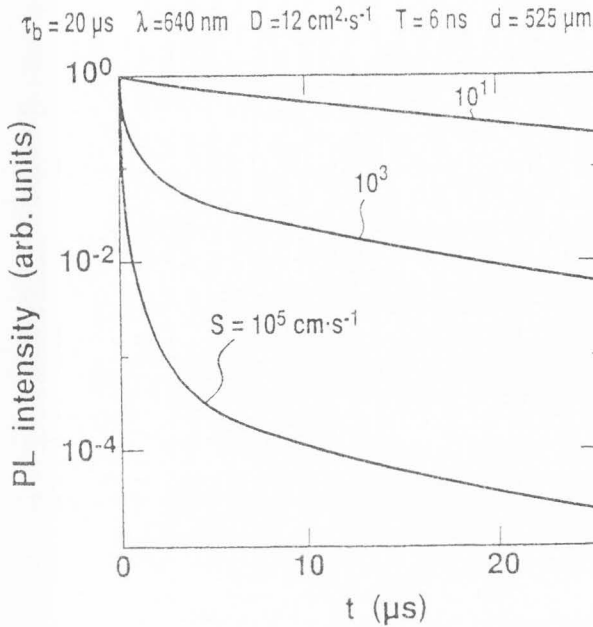


Figure 4. Simulated time changes of the depth profiles for the excess carrier densities ( $\Delta n$ ).

boxcar averager. Finally, the output from the boxcar is recorded on an X-Y recorder. To improve both the signal/noise ratio and the time response, the boxcar averager and the X-Y recorder were replaced by a digital oscilloscope and an X-Y plotter, respectively, at the final



**Figure 5.** Time decay curves of PL intensities for different values of  $S$ . PL intensities were assumed to be proportional to the absolute values of time derivatives for normalized excess carrier densities  $-dN_{\text{rel}}(t)/dt$ .

stage.

One-dimensional simulation was carried out by two methods on the assumption that the sample is under a low-excitation condition and that the ratio of radiative to non-radiative recombination rates is constant throughout the carrier decay process [5]. One method is to solve directly the diffusion equation with two boundary conditions, and the other is to employ the equations proposed by Buczkowski *et al.* [1], which were derived from the diffusion equation. The excess carrier density at specific position and time can only be obtained using the former method, whereas the normalized (averaged) excess carrier densities can be obtained using both methods. Therefore, the former was employed to obtain depth profiles for the excess carrier densities and the latter was employed to obtain time decay curves of the normalized excess carrier densities because the calculation time for the latter is much shorter than that for the former.

Equation (1) describes the one-dimensional diffusion equation whereas eqs. (2) and (3) represent boundary conditions.

$$\{\delta\Delta n(x,t)/\delta t\} = [D\{\delta^2\Delta n(x,t)/\delta x^2\}] - [\{\Delta n(x,t)\}/\tau_b] + G(x,t) \quad (1)$$

$$[D\{\delta\Delta n(x,t)/\delta x^2\}]|_{x=0} = S\Delta n(0,t) \quad (2)$$

$$[D\{\delta\Delta n(x,t)/\delta x^2\}]|_{x=d} = -S\Delta n(d,t) \quad (3)$$

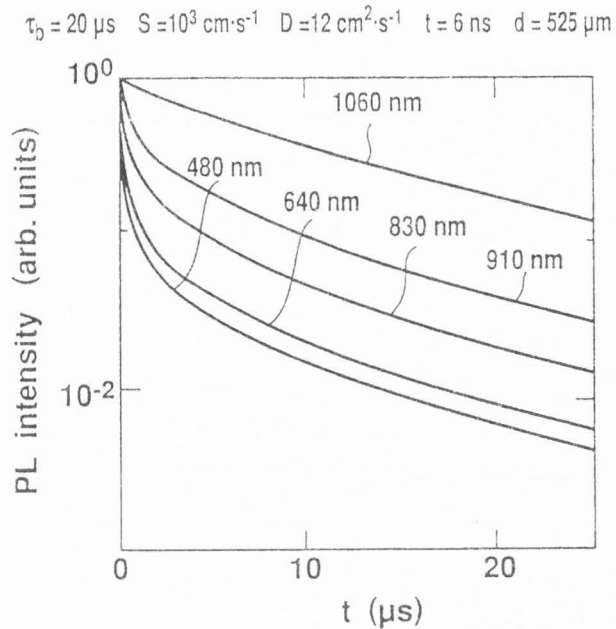


**Figure 6.** Time decay curves of PL intensities for different values of  $\lambda$ .

$\Delta n(x,t)$  shows the excess carrier density at position  $x$  in this one-dimensional model and at time  $t$  after the laser pulse is terminated.  $D$  represents the diffusion coefficient of Si crystals and is assumed here to be  $12 \text{ cm}^2/\text{s}$ . The wafer thickness is represented by  $d$  and is assumed here to be  $525 \mu\text{m}$ .  $G(x,t)$  represents the generated excess carrier density at position  $x$  and at time  $t$ . The laser pulse intensity is assumed to be of a rectangular shape with the pulse width  $T$ , which is fixed at  $6 \text{ ns}$ . Therefore,  $G(x,t)$  is expressed as:

$$G(x,t) = A \exp(-\alpha x) \text{ for } -T \leq t \leq 0; \\ = 0 \text{ for } T > 0 \quad (4)$$

where  $A$  is a constant and  $\alpha$  is the absorption coefficient of Si crystals which is assumed to be  $1.5 \times 10^4$ ,  $2.6 \times 10^3$ ,  $6.6 \times 10^2$ ,  $2.8 \times 10^2$  and  $1.2 \times 10^1 \text{ cm}^{-1}$  for the exciting wavelength ( $\lambda$ ) of 480, 640, 830, 910 and 1060 nm, respectively.  $S$  is assumed to be the same value for the two boundaries ( $x = 0$  and  $x = d$ ).

Equations (5), (6), (7), (8), (9) and (10) are those proposed by Buczkowski *et al.* [1].

$$N(\lambda,t) = \frac{8G_0 \exp(-\alpha_\lambda d/2)}{dT} \cdot \sum B_n(\lambda) \exp(-t/\tau_n) \quad (5)$$

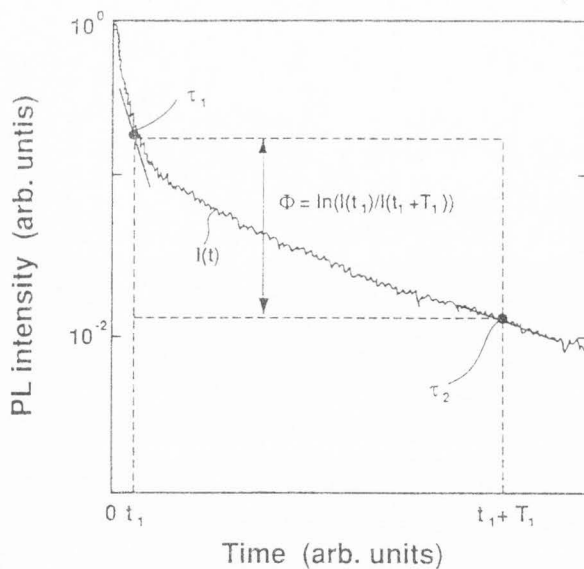


Figure 7. PL time decay curve and four parameters which were used in the curve-fitting algorithm.

$$N_{rel}(\lambda, t) = N(\lambda, t) / N(\lambda, 0) \quad (6)$$

$$B_n(\lambda) = \left\{ \frac{\sin(\alpha_n d/2) [1 - \exp(-T/\tau_n)]}{1/\tau_n (\alpha_\lambda^2 + \alpha_n^2) [\alpha_n d + \sin(\alpha_n d)]} \right\} \cdot \left\{ \alpha_\lambda \sinh \left[ \frac{\alpha_\lambda d}{2} \right] \cos \left[ \frac{\alpha_n d}{2} \right] + \alpha_n \cosh \left[ \frac{\alpha_\lambda d}{2} \right] \sin \left[ \frac{\alpha_n d}{2} \right] \right\} \quad (7)$$

$$1/\tau_n = \{1/\tau_b\} + \{1/\tau_{ns}\} \quad (8)$$

$$1/\tau_{ns} = \alpha_\lambda^2 D \quad (9)$$

$$F(\alpha) = (\alpha D/S) - \cot(\alpha d/2) \quad (10)$$

$N(\lambda, t)$  represents the averaged excess carrier density,  $G^0$  the generation function,  $\tau_n$  the  $n$ -th decay constant,  $\alpha_n$  the roots of  $F(\alpha)$  function, and  $\tau_{ns}$  the surface component of  $n$ -th decay constant.

### Results and Discussion

Figure 2 shows PL time decay curves for P-doped n-type Si wafers with a specific resistivity of 2.5  $\Omega$ cm

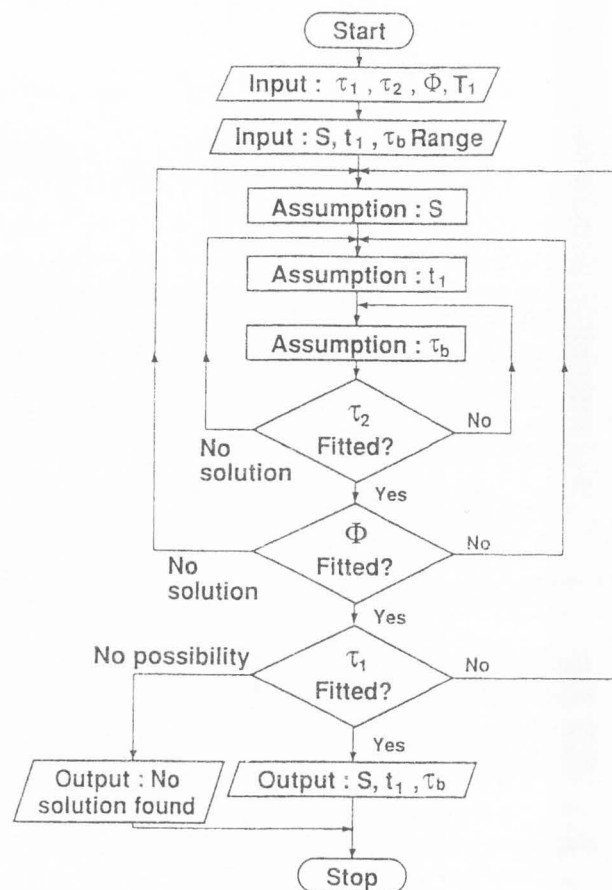


Figure 8. Simplified flow chart of the curve-fitting algorithm.

and a thickness of 525  $\mu$ m. Horizontal and vertical axes show the elapsed time after light from the dye laser is cut and the PM output on a linear scale, respectively. Dashed lines are baselines. The lower curve represents a mirrored wafer whose native oxide has been removed by dipping in HF solution, whereas the upper curve is for a sample where S has been reduced by dipping it in a reducing agent consisting of a SnCl<sub>2</sub> solution (2 wt%), after HF treatment. The PL time decay rate of the upper curve is low compared to that of the lower curve, which shows that the SnCl<sub>2</sub> treatment is effective in decreasing S for n-type crystals.

Figure 3 shows PL time decay curves for the same sample as in Figure 2, although here the vertical axis is plotted on a logarithmic scale. The decay rates are large in the early half and small in the latter half of the curves for both samples, a likely result of the fact that the pulsewidth of the laser light is very short compared with the carrier lifetime [7]. The carrier lifetimes obtained in the latter half are thought to be closer to  $\tau_b$  than those obtained in the first half. Because these excitation

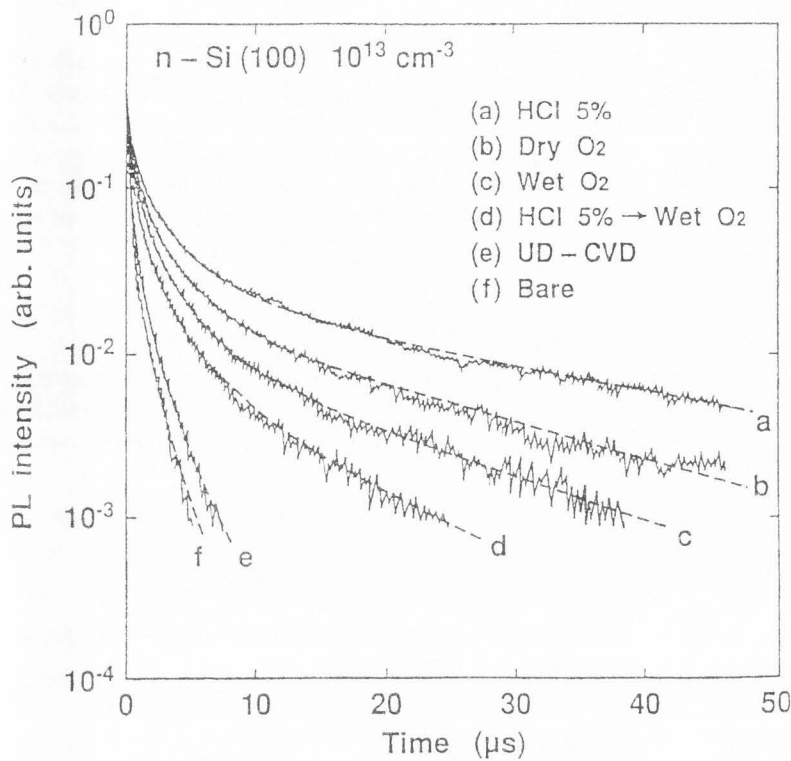


Figure 9. PL time decay curves of Si crystals covered with six kinds of  $\text{SiO}_2$ .

conditions appear to be low-injection ones, the effective minority carrier lifetimes ( $\tau_{\text{eff}}$ ), including  $\tau_b$  and  $S$ , are  $4.9 \mu\text{s}$  for the HF-treated sample and  $10 \mu\text{s}$  for the  $\text{SnCl}_2$  treated sample. Thus, it is demonstrated that it is very important to separate both  $\tau_b$  and  $S$  from  $\tau_{\text{eff}}$ . Therefore, simulation was carried out to develop an algorithm to obtain both parameters, which is based on the PL time decay measurement.

Figure 4 shows the simulated time changes of the depth profiles for the excess carrier density ( $\Delta n$ ). The vertical and horizontal axes are  $\Delta n$  and the relative wafer thickness, respectively. Elapsed times after a termination of the laser pulse are denoted in the figure. The values for  $\tau_b$ ,  $S$  and  $\lambda$  were assumed to be  $20 \mu\text{s}$ ,  $10^4 \text{ cm/s}$  and  $640 \text{ nm}$ , respectively.  $\Delta n$  decreased abruptly in the initial stage of the elapsed time because excess carriers were located only at the surface region and because they recombined at the surface very quickly due to the large value of  $S$ . However,  $\Delta n$  decreased slowly in the next stages of the elapsed time because excess carriers were located throughout the wafer and the effect of  $S$  was much less in these cases. The decrease of  $\Delta n$  towards the surface can be attributed to the large value of  $S$ . The peak position of  $\Delta n$  increased as the time elapsed, which can be attributed to the diffusion of excess carriers.

Figure 5 shows the time decay curves of PL intensities for different values of  $S$ . PL intensities were as-

sumed to be proportional to the absolute values of time derivatives for normalized carrier densities  $-dN_{\text{rel}}(t)/dt$  [5]. When the value of  $S$  became  $10^1 \text{ cm/s}$ , PL intensities decreased nearly exponentially. When the value of  $S$  became  $10^3$  or  $10^5 \text{ cm/s}$ , PL intensities decreased abruptly in the initial stage, followed by a rather slow exponential decrease. The increase of  $S$  affected especially the initial stages of time decay curves, resulting in their initial abrupt decreases.

Figure 6 shows time decay curves of PL intensities for different values of  $\lambda$ . When  $\lambda$  was  $1060 \text{ nm}$ , PL intensities decreased nearly exponentially, which means that the contribution of the surface recombination was very small in the cases of large values of  $\lambda$ , that is, small values of  $\alpha$ . As the values of  $\lambda$  became smaller, PL intensities began to decrease abruptly in the initial stages. Therefore,  $\lambda$  of  $640 \text{ nm}$  was used in the experiment to make it easier to obtain both  $\tau_b$  and  $S$ .

An initial abrupt decrease of the PL intensity is mainly determined by the value of  $S$  and the subsequent slow exponential decrease is determined by the values of both  $\tau_b$  and  $S$ . Based on this information, a curve-fitting algorithm has been developed to obtain both parameters. Figure 7 shows a PL decay curve and four parameters which were used in a curve-fitting algorithm.  $\tau_1$  is  $\tau_{\text{eff}}$  at time  $t_1$  in the initial stage and  $\tau_2$  is  $\tau_{\text{eff}}$  at time  $t_1 + T_1$  in the following stage. The exact value of  $t_1$  cannot be obtained because of the measuring system delay. There-

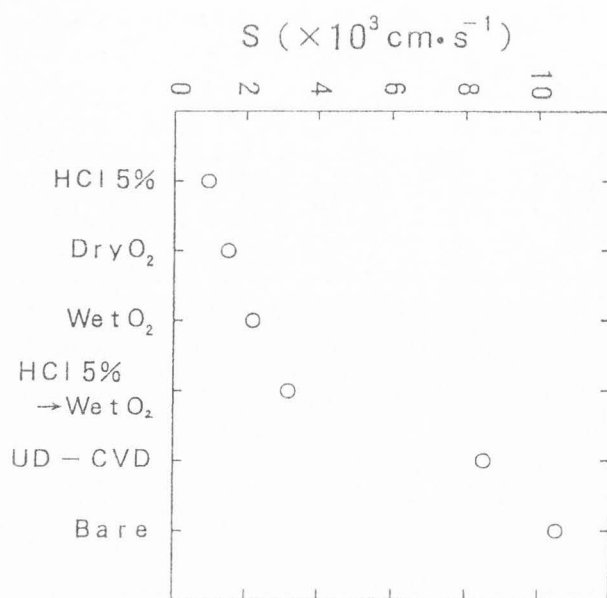


Figure 10. Values of  $S$  for six kinds of samples.

fore,  $t_1$  was not used as a parameter. The PL intensity at time  $t$  was defined as  $I(t)$ . Using that definition, the last parameter  $\Phi$  is defined by the following:

$$\Phi = \ln \left\{ \frac{I(t_1)}{I(t_1 + T_1)} \right\} \quad (11)$$

Figure 8 shows a simplified flow chart of the curve-fitting algorithm which was used to obtain both  $\tau_b$  and  $S$  from an experimental PL time decay curve. The algorithm starts with input of the four parameters  $\tau_1$ ,  $\tau_2$ ,  $\Phi$  and  $T_1$ . Secondly, the permitted ranges for  $S$ ,  $t_1$  and  $\tau_b$  are input. Within these ranges, the algorithm identifies the best-fitting values. Thirdly, the assumed values of  $S$ ,  $t_1$  and  $\tau_b$  are input for the calculation of the values for  $\tau_2$ ,  $\Phi$  and  $\tau_1$  which uses eqs. (5), (6), (7), (8), (9) and (10). Values of  $S$ ,  $t_1$  and  $\tau_b$  are varied repeatedly until an agreement between the input and calculated values of  $\tau_2$ ,  $\Phi$  and  $\tau_1$  is obtained. Only if there is a coincidence of all parameters,  $\tau_2$ ,  $\Phi$  and  $\tau_1$ , the values of  $S$ ,  $t_1$  and  $\tau_b$  are outputted.

Figure 9 shows PL time decay curves for Si crystals covered with six kinds of SiO<sub>2</sub>. Samples (a), (b), (c) and (d) were fabricated by oxidation in an HCl ambient, in a dry oxygen ambient, in a wet oxygen ambient, in a wet oxygen ambient after oxidation in an HCl ambient, respectively. The oxide of sample (e) was formed by chemical vapor deposition. No intentional oxidation was carried out for sample (f) although native oxide was formed on the surface. It was found that there were great differences in PL time decay curves although the six kinds of samples were fabricated from the same wafer lot, which means that there were great differences in

the values of  $S$  among the samples.

Figure 10 shows the values of  $S$  for all six kinds of samples. Samples (a), (b), (c), (d), (e) and (f) have  $S$  values of 950, 1500, 2200, 3200, 8300 and 10500 cm/s, respectively, although they have almost the same  $\tau_b$  values of 2001  $\mu$ s. These results indicate that PL time decay measurement is effective to obtain the values of  $\tau_b$  and  $S$ .

### Summary

A new method of PL time decay measurement for Si crystals has been presented to obtain both  $\tau_b$  and  $S$ . Good results were obtained for several wafers covered with SiO<sub>2</sub>.

### Acknowledgments

The authors would like to thank M. Azuma, H. Ohashi and Y. Uematsu for encouragement throughout this work.

### References

- [1] Buczkowski A, Radzimski ZJ, Rozgonyi GA, Simura F (1991) Bulk and surface components of recombination lifetime based on a two-laser microwave reflection technique. *J. Appl. Phys.* **69**, 6495-6499.
- [2] Luke KL, Cheng LJ (1987) Analysis of the interaction of a laser pulse with a silicon wafer: Determination of bulk lifetime and surface recombination velocity. *J. Appl. Phys.* **61**, 2282-2293.
- [3] Ogita Y (1990) Extended Abstracts, 90-1, The Electrochemical Society Meeting, Montreal, Canada, May 1990 (Electrochemical Society, Pennington, NJ) p. 702.
- [4] Orton JW, Blood P (1990) *The Electrical Characterization of Semiconductors, Measurement of Minority Carrier Properties*. Academic Press, San Diego. p. 6.
- [5] Thölmann K, Yamaguchi M, Yahata A, Ohashi H (1993) Simulation of time decay for photoluminescence emitted from silicon crystals excited by short laser pulse. *Jpn. J. Appl. Phys.* **32**, 1-6.
- [6] Wang CH, Neugroschel AN (1991) Minority-carrier lifetime and surface recombination velocity measurement by frequency-domain photoluminescence. *IEEE Trans. Electron Devices* **38**, 2169-2180.
- [7] Yahata A, Kuriki M (1992) Carrier lifetime depth profile for power devices with fast turn-on time investigated by photoluminescence decay method *Jpn. J. Appl. Phys.* **31**, 1758-1759.